Organic & Biomolecular Chemistry

ROYAL SOCIETY OF CHEMISTRY

PAPER

View Article Online
View Journal | View Issue

Open Access Article. Published on 02 October 2025. Downloaded on 2/8/2026 2:10:41 AM.
This article is licensed under a Creative Commons Attribution-NonCommercial 3.0 Unported Licence.

Check for updates

Cite this: *Org. Biomol. Chem.*, 2025, **23**, 9380

Combining photocatalysis with imine reductases to access stereodefined pyrrolidines from oxime benzoates

Stefano Parisotto, * Marco Blangetti and Cristina Prandi

In this paper, we present the first combination of commercially available imine reductases (IREDs) with the photocatalytic hydroimination of alkene-tethered iminyl radicals. Notably, the photochemical step was achieved from simple oxime benzoates lacking additional electron-withdrawing activation. This hybrid cascade enabled the synthesis of diverse 2,5-disubstituted pyrrolidines with good functional group compatibility and tolerance to sterically demanding substrates. Additionally, our methodology was extended to the preparation of a novel *all cis* analogue of (–)-codonopsinine. Mechanistic studies suggested the generation of the key iminyl radical from the benzoate by triplet–triplet energy transfer (TTE_nT).

Received 1st September 2025,
Accepted 1st October 2025

DOI: 10.1039/d5ob01407g

rsc.li/obc

Introduction

One-pot cascade and telescoped reactions are an increasingly active area of research, offering a more streamlined approach to chemical synthesis. By combining multiple catalytic steps into a single reaction vessel, these processes eliminate intermediate manipulations, not only reducing waste production but also saving time, particularly when all catalysts and reagents are added from the beginning, as in tandem reactions. Although many successful cascades have been developed within individual catalytic domains, such as organo-,[1] bio-,[2] or photocatalysis,[3] combining catalysts across these fields remains a significant challenge due to compatibility issues. This occurs especially when enzymes are involved as they operate mostly in aqueous solutions at room temperature and controlled pH to preserve enzyme stability and activity. Addressing these compatibility issues unlocks possibilities for building complex molecules through hybrid catalytic systems. In this scenario the combination of biocatalysis with photochemistry has gained attention, particularly in the last decade.[4] Indeed, while photocatalysis produces valuable synthetic intermediates and reactive species under reaction conditions compatible with most enzymes, biocatalysis exploits highly specific enzymes to catalyse reactions with superior chemo- and stereoselectivity. Such tandem photocatalyst/enzyme reactions have largely been exploited for the stereocontrolled synthesis of α-chiral alcohols and amines (Scheme 1a).[5] These transformations typically involve the photocatalytic generation of prochiral ketones, subsequently converted into optically active products by alcohol dehydrogenases (ADHs),[6–10] or transaminases (TAs).[11–14] However, the formation of more structurally complex scaffolds such as saturated nitrogen heterocycles has been far less explored and only one example has been reported where the photocatalytic reduction of pyrrolines was combined with monoamine oxidases (MAOs).[15] Imine reductases (IREDs) have recently

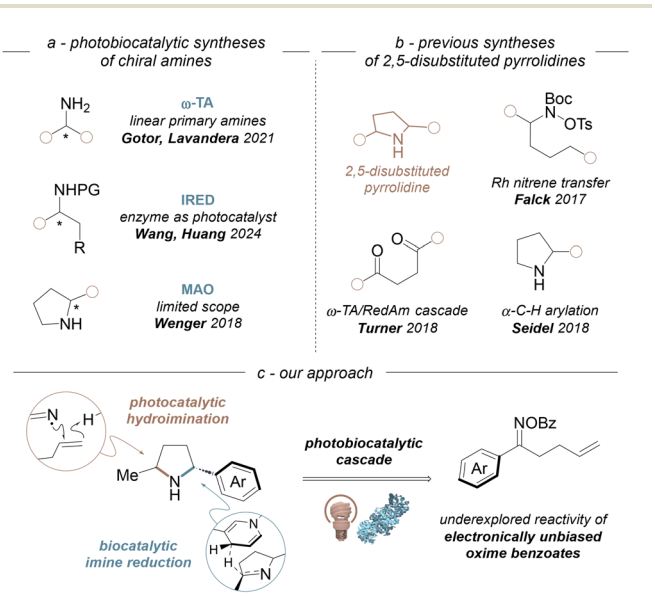

Scheme 1 (a) Known photobiocatalytic syntheses of chiral amines; (b) selected methodologies to access chiral 2,5-disubstituted pyrrolidines; (c) our designed photobiocatalytic cascade.

Dipartimento di Chimica, Università di Torino, Via Pietro Giuria 7, 10125 Torino, Italy. E-mail: stefano.parisotto@unito.it

This journal is © The Royal Society of Chemistry 2025

Open Access Article. Published on 02 October 2025. Downloaded on 2/8/2026 2:10:41 AM. This article is licensed under a Creative Commons Attribution-NonCommercial 3.0 Unported Licence.

emerged as highly versatile biocatalysts for the synthesis of cyclic secondary amines.[16,17] Their versatility, substrate tolerance, and high stereoselectivity have made them attractive candidates for the integration into hybrid catalytic systems. Several research groups have explored such approaches: Lipshutz combined IREDs with palladium catalysis,[18] while Turner has reported hybrid systems involving organolithium reagents,[19] electrocatalysis,[20] and Lewis acid catalysis.[21] Yet, despite this growing interest, no photobiocatalytic cascades have been reported to date employing IREDs.

In the context of our ongoing interest in using imine reductases under non-conventional conditions,[22] we recently focused our attention on their integration with photocatalysis. Since several methodologies involving visible light have been reported for the synthesis of substituted pyrrolines,[23] we envisioned that their combination with imine reductases could provide a new route to cyclic amines and in particular to 2,5-disubstituted pyrrolidines (Scheme 1c), commonly found in the core structure of organocatalysts,[24] bioactive compounds,[25] and natural alkaloids.[26] This methodology would complement existing approaches (Scheme 1b) such as the direct C–H functionalisation of pyrrolidines using organolithiums reported by Seidel,[27] the rhodium-catalysed nitrene transfer with *N*-tosyloxycarbamates,[28] and the multienzymatic cascades combining transaminases with monoamine oxidases,[29] or imine reductases.[30] Notably, although Wang and Huang recently demonstrated the use of IREDs in photobiocatalysis for the stereoselective addition of alkyl radicals to enamides,[31] no photobiocatalytic cascades involving imine reductases have been hitherto reported. Among the several photochemical transformations leading to cyclic imines, we focused on the hydroimination of alkene-tethered iminyl radicals. These reactive species are typically generated *via* N–O bond cleavage in oxime esters or ethers, often requiring electron-deficient substrates to enable efficient reduction by the photocatalyst's excited-state. So far, this approach has heavily relied on aromatic rings bearing strong electron-withdrawing groups (*e.g.*, $-NO_2$,[32] $-CF_3$,[33,34] $-F$[35]) to enhance redox activity. In contrast, we were interested in investigating the use of simple oxime benzoates lacking additional electron-withdrawing activation.

Results and discussion

At the onset of our study, we evaluated the reactivity of **2a** in a photocatalytic hydroimination, with the results reported in Table 1. Anticipating the difficult single-electron reduction of simple benzoates, we selected *fac*-Ir(ppy)$_3$ (**PC-1**) for its strong reducing potential in both oxidative and reductive quenching cycles ($E_0(PC^*/PC^+) = -1.73$ V, $E_0(PC/PC^-) = -2.19$ V).[36] As the hydrogen atom donor, we used γ-terpinene (**HAT-1**). Upon blue-light irradiation of a 0.1 M solution of **2a** in DMF, we observed complete conversion of the starting material after 24 hours and a 64% yield of pyrroline **3a** (entry 1). The unexpected result pointed out that the desired reactivity could indeed be unlocked from the simple benzoate, without the need to use electron-deficient benzoic acid derivatives. Given the encouraging starting point and attributing the moderate yield to an inefficient hydrogen abstraction by the intermediate carbon-centred primary radical, we screened alternative hydrogen atom donors. Using triethylsilane, triisopropylsilanethiol, and Hantzsch ester (**HAT-2**, **HAT-3** and **HAT-4**, entries 2–4) we obtained only trace amounts of the desired product. Based on our initial reaction design (see Scheme S1 in SI), we reasoned that after hydrogen atom transfer from γ-terpinene, the cyclohexadienyl radical could readily aromatise to *p*-cymene (a by-product detected by GC MS and ^{1}H NMR) thus facilitating the photocatalyst turnover.

To probe the role of the aromatisation, we tested cycloheptatriene, which can similarly aromatise to a tropylium ion. This gave low conversion of **2a** (65% unreacted **2a**) and moderate yield of **3a** (entry 6). Triphenylmethane also proved effective (60% yield, entry 5), which we attributed to both the stability of the trityl cation and its comparable hydrogen-donating ability (BDE triphenylmethane = 81 kcal mol^{-1},[37] *vs.* BDE γ-terpinene ≈ 77 kcal mol^{-1}).[38] Surprisingly, we later found out that 4CzIPN (**PC-2**) catalysed the reaction with similar efficiency to the iridium complex (61% yield, entry 7), whereas other catalysts were not effective. Hence, **PC-2** was chosen as elective catalyst to carry on with the optimisation of the reaction conditions. The solvent played a crucial role in improving the yield of the hydroimination. Indeed, we got optimal results by replacing DMF with acetone and increasing the intensity of the light source (82% yield, entry 12). CPME also outperformed DMF (72% yield, entry 17) and promising results were obtained even in water (50% yield and 67% conversion, entry 8). Aiming at a one-pot photobiocatalytic cascade we repeated the reaction in phosphate buffer; however, we recovered a complex reaction mixture suggesting complete decomposition of **2a**. Finally, although a slight increase in the yield was observed in the presence of K_2CO_3 (85% yield, entry 25), we chose not to include it to maintain a less complex reaction medium and minimise potential interferences in the subsequent enzyme-catalysed step. No further improvement was observed changing the molarity of the reaction (entries 15–17), nor the loading of the HAT reagent (entries 18–20). Next, we conducted control experiments to confirm the role of each component in the reaction mixture (Table 2). Quantitative recovery of unreacted oxime benzoate **2a** after conducting the reaction in the dark or in the absence of 4CzIPN confirmed the photocatalytic nature of the reaction (entries 1 and 2). The role of γ-terpinene as the hydrogen radical source was supported by the reduced efficiency observed in its absence, with imine **3a** still forming in 25% yield (entry 3). To assess whether the solvent might participate in the HAT step, we repeated the reaction in deuterated acetone. The reaction proceeded with similar yield, and the product (***d*-3a**) showed 30% deuterium incorporation at the exocyclic methyl group, supporting the participation of the solvent in the process, either through direct hydrogen donation or *via* hydrogen/deuterium exchange with an intermediate donor species. Moreover, when the model reaction

Open Access Article. Published on 02 October 2025. Downloaded on 2/8/2026 2:10:41 AM. This article is licensed under a Creative Commons Attribution-NonCommercial 3.0 Unported Licence.

Table 1 Optimisation of the photocatalytic hydroimination of oxime benzoate **2a** to afford pyrroline **3a**

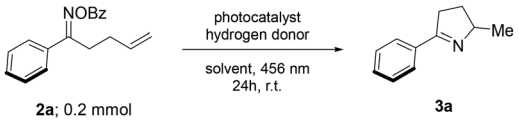

2a; 0.2 mmol — **3a**

Entry	Photocatalyst	Hydrogen donor (eq.)	Solvent	Yield **3a**[a] (%)
1	**PC-1**	**HAT-1** (2.0 eq.)	DMF [0.1 M]	64
2	**PC-1**	**HAT-2** (2.0 eq.)	DMF [0.1 M]	Traces
3	**PC-1**	**HAT-3** (2.0 eq.)	DMF [0.1 M]	Traces
4	**PC-1**	**HAT-4** (2.0 eq.)	DMF [0.1 M]	Traces
5	**PC-1**	**HAT-5** (2.0 eq.)	DMF [0.1 M]	60
6	**PC-1**	**HAT-6** (2.0 eq.)	DMF [0.1 M]	23 (65 **2a**)
7	**PC-2**	**HAT-1** (2.0 eq.)	DMF [0.1 M]	61
8[b]	**PC-2**	**HAT-1** (2.0 eq.)	H_2O [0.1 M]	56 (23 **2a**)
9	**PC-2**	**HAT-1** (2.0 eq.)	NaPi pH 8 [0.1 M]	0
10	**PC-2**	**HAT-1** (2.0 eq.)	CH_3CN [0.1 M]	24 (73 **2a**)
11	**PC-2**	**HAT-1** (2.0 eq.)	Acetone [0.1 M]	50 (35 **2a**)
12[c]	**PC-2**	**HAT-1 (2.0 eq.)**	**Acetone [0.1 M]**	**82**
13[d]	**PC-2**	**HAT-1** (2.0 eq.)	Acetone [0.1 M]	78
14[e]	**PC-2**	**HAT-1** (2.0 eq.)	Acetone [0.1 M]	76
15	**PC-2**	**HAT-1** (2.0 eq.)	Acetone [0.2 M]	79
16	**PC-2**	**HAT-1** (2.0 eq.)	Acetone [0.05 M]	74
17	**PC-2**	**HAT-1** (2.0 eq.)	CPME [0.1 M]	72
18	**PC-2**	**HAT-1** (1.0 eq.)	Acetone [0.1 M]	75 (5 **2a**)
19	**PC-2**	**HAT-1** (1.5 0 eq.)	Acetone [0.1 M]	78
20	**PC-2**	**HAT-1** (4.0 eq.)	Acetone [0.1 M]	80
21	**PC-1**	**HAT-1** (2.0 eq.)	Acetone [0.1 M]	67
22	**PC-3**	**HAT-1** (2.0 eq.)	Acetone [0.1 M]	0 (84 **2a**)
23	**PC-4**	**HAT-1** (2.0 eq.)	Acetone [0.1 M]	50 (38 **2a**)
24[f]	**PC-5**	**HAT-1** (2.0 eq.)	Acetone [0.1 M]	0 (99 **2a**)
25[g]	**PC-2**	**HAT-1** (2.0 eq.)	acetone [0.1 M]	85

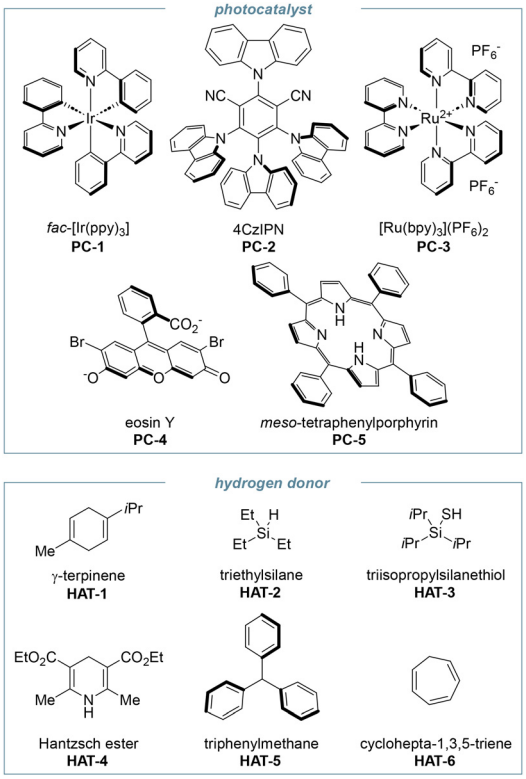

[a] Yield determined by ^{1}H NMR using 1,3,5-trimethoxybenzene as the internal standard. [b] Stirring was conducted at 1500 rpm to obtain a dispersion of droplets. [c] The intensity of the light source (Kessil lamp) was increased from 50% to 75%. [d] The intensity of the light source (Kessil lamp) was increased from 50% to 100%. [e] The intensity of the light source (Kessil lamp) was increased from 50% to 100% and the reaction time was reduced to 16 hours. [f] Under red-light irradiation by a 660 nm LED chip. [g] 1.0 equivalent of K2CO3 was added.

was performed in the presence of radical quenchers, such as TEMPO and BHT, the formation of radical adducts **3a-TEMPO** and **3a-BHT** confirmed the radical nature of the transformation (entries 5 and 6). Moreover, the reaction was conducted under aerated condition, by saturating the reaction vessel with oxygen prior to irradiation. After 24 hours we recovered a complex reaction mixture containing unreacted oxime benzoate **2a** (23%) and imine **3a** (31%, entry 7). Removal of the photocatalyst and irradiation using 370 nm LEDs provided the desired product in a low 27% yield (entry 8), thus confirming the beneficial role of 4CzIPN in mediating the photochemical reaction.

Having established the optimal conditions for the photochemical step, we selected imine **3f** and screened a set of commercially available imine reductases to identify the most suitable enzyme for the desired transformation. The results are summarised in Scheme 2a. Using our previously optimised conditions,[22] a suspension of pyrroline **3f** (0.1 M) in a sodium phosphate buffer (pH 8)/glycerol mixture was treated with different IREDs. $NADP^+$ was employed as the cofactor and regenerated *in situ* using glucose dehydrogenase (GDH-101) and D-glucose. After 48 hours, full conversion was observed only with two variants, IRED-44, and IRED-72, yielding pyrrolidine **4f** in 78% and 82% yield, respectively. IRED-69 also showed good catalytic activity (53% yield, 80% conversion), while IRED-17, IRED-18, and IRED-33 gave only low to moderate conversion. The reduction proceeded with excellent (*S*)-stereoselectivity, consistent with previous reports, yielding **4f** as a mixture of diastereomers. At higher conversions, equimolar mixtures of *cis* and *trans* isomers were obtained. In contrast, the limited activity of IRED-17, -18, and -33 resulted in partial kinetic resolution, favouring the formation of the *cis* isomer. Given the optimal performance of IRED-44, we assessed its compatibility with the photocatalytic process by evaluating the effect of individual reagents and major by-products from the hydroimination step (Scheme 2b). No signifi-

 This journal is © The Royal Society of Chemistry 2025

Open Access Article. Published on 02 October 2025. Downloaded on 2/8/2026 2:10:41 AM. This article is licensed under a Creative Commons Attribution-NonCommercial 3.0 Unported Licence.

Table 2 Control experiments on the photocatalytic hydroimination of oxime benzoate **2a**

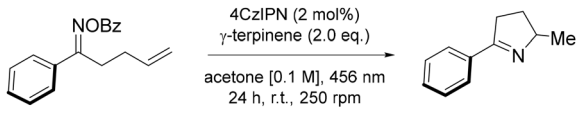

2a; 0.2 mmol **3a**: 82%

Entry	Deviation	Yield **3a**[a] (%)
1	Reaction conducted in the dark	0 (99 **2a**)
2	No photocatalyst	0 (99 **2a**)
3	No γ-terpinene	25
4	Reaction carried out in acetone-*d*6	23 (**3a** : **d**-**3a** 7 : 3)
5[b]	TEMPO (1.0 eq.) added	Traces (>90 **2a**)
6[d]	BHT (1.0 eq.) added	41[c] (14 **2a**)
7	Aerated conditions	31 (23 **2a**)
8	No photocatalyst, 370 nm	27

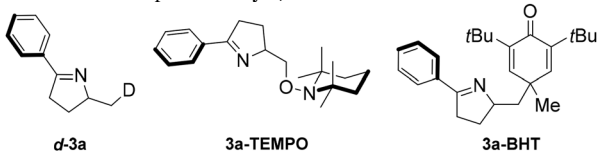

d-**3a** **3a-TEMPO** **3a-BHT**

[a] Yield determined by ^{1}H NMR using 1,1,2,2-tetrachloroethane as the internal standard unless otherwise specified. [b] **3a-TEMPO** detected by HRMS analysis. [c] Isolated yield. [d] **3a-BHT** detected by HRMS analysis.

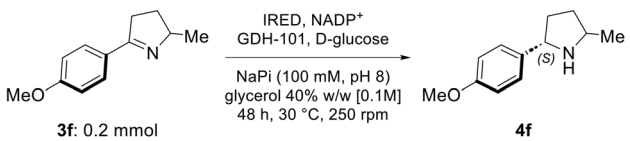

3f: 0.2 mmol **4f**

a - catalytic performance of commercial IREDs

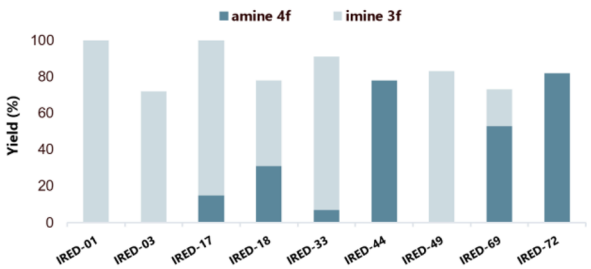

b - IRED-44 robustness

entry	additive	conv. 3f (%)[a]	yield 4f (%)[a]	dr[b]	er[c]
1	-	>99	78	1:1	>99:1
2	γ-terpinene	>99	74	1:1	>99:1
3	*p*-cymene	>99	76	1:1	>99:1
4	4CzIPN	>99	80	1:1	>99:1
5	BzOH	66	65	1:1.2	>99:1
6[d]	BzOH	>99	77	1:1	>99:1

Scheme 2 Biocatalytic reduction of imine **3f**. (a) screening of commercial IREDs; (b) **3f** reduction if the presence of potential inhibitors.

cant inhibition was observed upon the addition of γ-terpinene, *p*-cymene, or 4CzIPN (entries 2–4). However, the addition of one equivalent of benzoic acid significantly reduced the conversion of pyrroline **3f** (entry 5), likely due to a drop of the pH below the optimal range for this enzyme (7.0–8.5 as reported by the supplier). Increasing the volume of the buffer solution mitigated this effect (entry 6), and we therefore optimised the biocatalytic step by conducting the reduction at a final substrate concentration of 75 mM.

Finally, with the aim of producing stereodefined pyrrolidines directly from oxime benzoates, we developed a one-pot cascade process integrating the photochemical and biocatalytic steps. As mentioned before, initial attempts to perform the photochemical reaction on oxime benzoate **2a** in phosphate buffer failed to yield the desired pyrroline **3a**, ruling out a fully concurrent cascade. However, by conducting the photochemical step in acetone, we enabled a sequential (telescoped) cascade process. Indeed, a rapid solvent switch from volatile acetone to the aqueous phosphate buffer containing all components required for biocatalysis allowed smooth progression to the biocatalytic reduction. The designed cascade was first applied to model substrate benzoate **2a**, and we were pleased to observe complete conversion of both the starting material and the intermediate imine, yielding the desired amine **4a** in 64% yield with the expected diastereoselectivity (dr 1 : 1) and excellent enantioselectivity in the biocatalytic step (er >99 : 1 for both diastereomers). Furthermore, a ten-fold scale-up of the reaction was successfully carried out, affording product **4a** in 49% yield with same selectivity. Notably, the use of a fed-batch strategy in the biocatalytic step (see SI for a detailed procedure) enabled a tenfold increase in the enzyme-to-substrate ratio without a significant drop in the overall yield. To demonstrate the versatility of the developed hybrid process, we applied it to a selection of oxime benzoates **2a–o** featuring different substituents, including electron-rich and electron-poor arenes, heteroarenes, and substituted scaffold (Scheme 3).

The desired pyrrolidines **4a–o** were isolated with high stereoselectivity (er >99 : 1) and modest to good yields (40–72%). The photobiocatalytic reaction tolerated a moderate range of substituted arenes. Halogenated substrates were all successfully converted into products **4b–d**, highlighting the compatibility of the cascade with synthetically versatile and reactive handles. We obtained good yields for fluorinated products **4d** (*p*-F phenyl) and **4e** (*p*-CF_3 phenyl), which are especially significant in the context of pharmaceutical chemistry, where fluorine incorporation is widely employed to enhance metabolic stability, membrane permeability, and target binding affinity. Substrates bearing electron-donating groups, such as the methoxy and methyl group, were also well tolerated, providing good yields for products **4f–g** (up to 70%), confirming that the electronic nature of the aryl group has minimal impact on the efficiency of the hybrid process. To probe the steric constraints of the enzymatic reduction step, we evaluated the preparation of *ortho*-substituted arene **4h** and the naphthyl derivative **4i**. These bulkier substrates led to

Open Access Article. Published on 02 October 2025. Downloaded on 2/8/2026 2:10:41 AM.
This article is licensed under a Creative Commons Attribution-NonCommercial 3.0 Unported Licence.

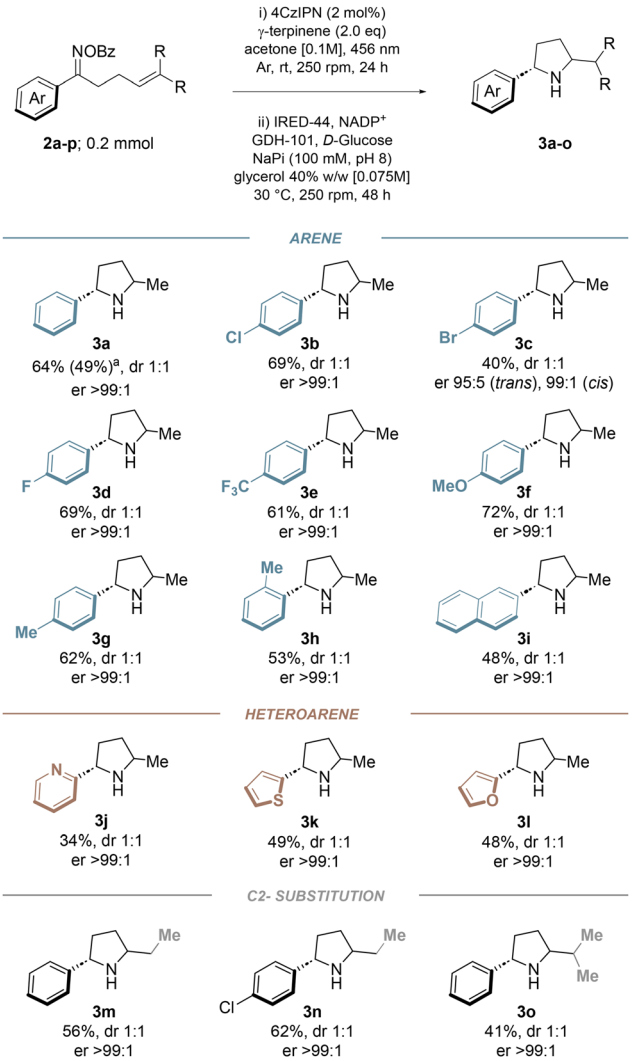

Scheme 3 Scope of the photobiocatalytic synthesis of pyrrolidines **4a–o** from oxime benzoates **2a–o**.

slightly diminished yields (53% and 48%, respectively), suggesting some sensitivity to steric hindrance near the imine moiety, yet the reaction remained viable, reflecting the remarkable substrate flexibility of the IRED. We further examined heteroaryl-derived substrates, which are prominent in drug and agrochemical discovery. 2-Pyridyl (**4m**), 2-thienyl (**4n**), and 2-furyl (**4o**) analogues were all successfully isolated (34–49% yield), confirming the compatibility of the process with heteroatom-containing substrates, which often present challenges in both photocatalysis and biocatalysis. Finally, to assess the enzyme's tolerance to substitutions on the pyrroline ring, we introduced larger alkyl groups at the 2-position. While ethyl-substituted products (**4m**, **4n**) were obtained in good yields (up to 62%), the more sterically demanding isopropyl derivative afforded a reduced yield for product **4o** (42%). Given the good functional group compatibility and the moderate tolerance towards larger substituent on the azacycle, we applied the photobiocatalytic methodology to the preparation of an analogue of codonopsinine. This alkaloid which was first isolated from *Codonopsis clematidea* by Matkhalikova and co-workers in 1969,[39] features a 1,2,3,4,5-pentasubstituted pyrrolidine core bearing a *p*-anisyl group at the C2-position. This natural product has attracted interest due to its biological properties, including antibiotic and hypotensive effects.[40] Its epimer, 4-*epi*-codonopsinine, exhibits inhibitory activity against α-fucosidase,[41] moreover both natural codonopsinine and its synthetic derivatives have shown promising activity against methicillin-resistant *Staphylococcus aureus* (MRSA).[42] In this context, we prepared oxime benzoate **2p** from D-ribose (see SI for the full synthetic route) and subjected it to our optimised photobiocatalytic protocol, producing pyrrolidine **4p** as a single stereoisomer in 44% yield (Scheme 3). As mentioned before, all previous products were generated as a mixture of enantiopure diastereomers, owing to the inherent non-selective photochemical cyclisation that produced racemic imines. However, employing oxime benzoate **2p**, which features two consecutive chiral centers derived from ribose, alongside the rigidity induced by the cyclic ketal moiety, the photocatalytic step becomes stereoselective. This results in the enzymatic reduction yielding a single stereoisomer of the final pyrrolidine. This result highlights the potential of this methodology, which complements recent advances in the biocatalytic preparation of bioactive imino- and aminosugars,[43,44] to access a new class of *all cis* codonopsinine analogues, thereby expanding the accessible chemical space for future biological exploration.

Finally, given the unexpected results observed with simple oxime benzoates despite the mild reducing ability of 4CzIPN, we hypothesised that the photochemical step might be initiated by triplet–triplet energy transfer rather than by single electron transfer. Oxime benzoate **2a** exhibits two reduction peaks (Scheme 5b): at −1.70 V and −2.32 V, relatively far from the redox properties of the catalyst ($E_0(PC^*/PC^+)$ = −1.18 V, $E_0(PC/PC^-)$ = −1.24 V).[45] Due to their desirable photophysical properties, carbazolyl benzonitriles have been used also in photochemical transformations involving Dexter triplet–triplet

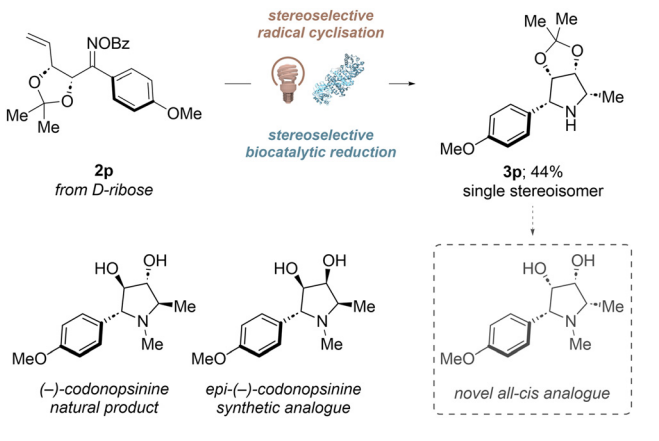

Scheme 4 Photobiocatalytic approach toward a novel *all cis* analogue of (–)-codonopsinine.

This journal is © The Royal Society of Chemistry 2025

Open Access Article. Published on 02 October 2025. Downloaded on 2/8/2026 2:10:41 AM. This article is licensed under a Creative Commons Attribution-NonCommercial 3.0 Unported Licence.

a - catalytic performance of photocatalysts

entry	PC	E_T (kcal·mol^{-1})	$E_{1/2}^{[PC+]/[PC*]}$ (V)	yield 3a (%)[a]
1	4CzIPN	57.1	-1.04	82
2	*fac*-Ir(ppy)$_3$	58.1	-1.73	67
3	eosin Y	45.4	-1.11	50
4	[Ru(bpy)$_3$](PF$_6$)$_2$	49.0	-0.81	0
5	H_2TPP	33.0	-0.42	0
6	Benzil	53.3	n.d.	6
7	Michler's ketone	61.0	-1.84	33
8[b]				68
9	Thioxanthone	65.5	-1.18	14
10[b]				0

[a] yield determined by ^{1}H NMR using 1,3,5-trimethoxybenzene as the internal standard.
[b] under irradiation at 390 nm.

*b - CV of **2a***

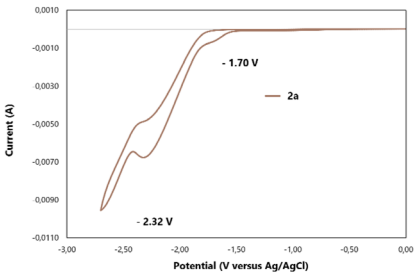

c - mechanism proposal

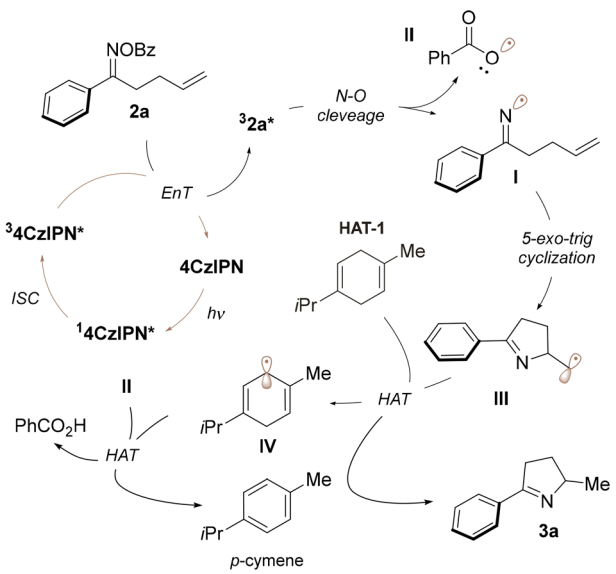

Scheme 5 (a) Catalytic performance of different photocatalyst in the conversion of oxime benzoate **2a**; (c) electrochemical characterization of oxime benzoate **2a**; (b) mechanistic investigation on the iminyl radical formation and proposed catalytic cycle for N–O cleavage and hydroimination.

energy transfer (TTE$_n$T).[46,47] As the triplet state energy for 4CzIPN is 58.3 kcal mol^{-1},[48] derivatives with a lower energy should undergo photosensitisation. Taking advantage of the machine-leaning platform recently developed by Glorius,[49] we calculated a value of 56.08 kcal mol^{-1} for the energy of the triplet state of **2a**. Comparing this value with those of 4CzIPN and the photocatalysts we tested, we observed a good correlation with the results observed during the optimisation (Scheme 5a). In addition, we also tested other organic sensitizers and got stronger evidence of an energy transfer process (Scheme 4). While benzyl (E_T = 53.3 kcal mol^{-1}) afforded minimal conversion (entry 6), Michler's ketone (E_T = 61.0 kcal mol^{-1}) produced imine **3a** with 33% yield and 35% conversion. Notably, both conversion and yield improved (86% and 68% respectively) upon irradiating the reaction mixture at 390 nm to better match the spectroscopic feature of the sensitizer (entries 7 and 8 respectively). Also, thioxanthone (E_T = 65.5 kcal mol^{-1}) was tested under blue and purple light. In the former experiment we observed low conversion (22%) and 14% yield (entry 9). Switching to purple light resulted in the complete conversion of oxime benzoate **2a**, but no product could be detected in the crude mixture, suggesting a possible degradation of the product (entry 10).

Based on these results and on the experiments summarised in Table 2, we are inclined to propose that following the photoexcitation of 4CzIPN to its singlet state (^{1}**4CzIPN***) and its successive interconversion into triplet state (^{3}**4CzIPN***), the reaction is initiated upon sensitisation of oxime benzoate **2a** to ^{3}**2a*** *via* energy transfer (Scheme 5c). Homolysis of the N–O bond produces iminyl radical **I** and benzyloxy radical **II**. Exocyclic radical **III** is then produced upon 5-*exo*-trig cyclisation, which abstracts a hydrogen atom from γ-terpinene producing imine **3a** and bis-allyl radical **IV**. The latter finally aromatises to *p*-cymene by a second hydrogen atom transfer, producing benzoic acid from radical **II**.

Conclusions

In summary, the biocatalytic activity of commercially available imine reductases has been integrated for the first time with the photocatalytic hydroimination of alkene-tethered oxime esters. Remarkably, we demonstrated the possibility to employ simple oxime benzoates lacking additional electron-withdrawing activation. Experimental mechanistic studies revealed that the key iminyl radical might be produced *via* triplet–triplet energy transfer from such benzoates. This novel cascade allowed the preparation of a selection of different 2,5-disubstituted pyrrolidines, showing good functional group compatibility and tolerance towards sterically demanding substrates. Moreover, the commercial IREDs retained catalytic activity under the non-conventional conditions of the hybrid process, including in the presence of potentially inhibitory photochemical by-products. This robustness broadens the accessibility of biocatalysis, offering a practical route even for chemists without access to enzyme expression or protein engineering facilities. Finally, the pre-

Open Access Article. Published on 02 October 2025. Downloaded on 2/8/2026 2:10:41 AM. This article is licensed under a Creative Commons Attribution-NonCommercial 3.0 Unported Licence.

sented methodology was applied to the preparation of a novel *all cis* analogue of (−)-codonopsinine.

Author contributions

All authors have given approval to the final version of the manuscript. The manuscript was written through contributions of all authors. Stefano Parisotto (conceptualization, methodology, investigation, visualization, writing – original draft, writing review and editing), Marco Blangetti (funding acquisition, writing review and editing), and Cristina Prandi (conceptualization, funding acquisition, project administration, supervision, writing – review & editing).

Conflicts of interest

There are no conflicts to declare.

Data availability

The data supporting this article have been included as part of the supplementary information (SI). Supplementary information is available. See DOI: **https://doi.org/10.1039/d5ob01407g**.

Acknowledgements

This work was carried out under the framework of the project NODES which has received funding from the MUR – M4C2 1.5 of PNRR with grant agreement no. ECS00000036. Authors acknowledge support from the Project CH4.0 under the MUR program "Dipartimenti di Eccellenza 2023-2027" (CUP: D13C22003520001). This research was also supported by EU funding within the MUR PNRR Extended Partnership initiative on Emerging Infectious Diseases (Project no. PE00000007, INF-ACT). We are grateful to Dr Francesco Pellegrino for assistance in electrochemical analysis and data interpretation and to Dr Federica De Nardi for support in the use of enzymes and for fruitful discussions on biocatalysis.

References

1 C. Grondal, M. Jeanty and D. Enders, *Nat. Chem.*, 2010, **2**, 167–178.
2 E. Grandi, F. Feyza Özgen, S. Schmidt and G. J. Poelarends, *Angew. Chem., Int. Ed.*, 2023, **62**, e202309012.
3 D. Liang, Q.-Q. Zhou and J. Xuan, *Org. Biomol. Chem.*, 2024, **22**, 2156–2174.
4 M. A. Emmanuel, S. G. Bender, C. Bilodeau, J. M. Carceller, J. S. DeHovitz, H. Fu, Y. Liu, B. T. Nicholls, Y. Ouyang, C. G. Page, T. Qiao, F. C. Raps, D. R. Sorigué, S.-Z. Sun, J. Turek-Herman, Y. Ye, A. Rivas-Souchet, J. Cao and T. K. Hyster, *Chem. Rev.*, 2023, **123**, 5459–5520.
5 S. Parisotto and C. Prandi, *Adv. Synth. Catal.*, 2025, 03.
6 S. Filgueira, L. Rodríguez-Fernández, I. Lavandera and V. Gotor-Fernández, *ChemSusChem*, 2025, 2500683.
7 A. Rudzka, N. Antos, T. Reiter, W. Kroutil and P. Borowiecki, *ACS Catal.*, 2024, **14**, 1808–1823.
8 Y. Liu, K. Zhu, X. Li, X. Wu, J. Feng, A. Roosta, Q. Wu and D. Zhu, *Tetrahedron Chem*, 2024, **11**, 100083.
9 J. Wang, Y. Peng, J. Xu and Q. Wu, *Org. Biomol. Chem.*, 2022, **20**, 7765–7769.
10 F. F. Özgen, A. Jorea, L. Capaldo, R. Kourist, D. Ravelli and S. Schmidt, *ChemCatChem*, 2022, **14**, e202200855.
11 M. Logotheti, S. Gehres, A. S. França, U. T. Bornscheuer, R. O. M. A. de Souza and M. Höhne, *J. Org. Chem.*, 2025, **90**, 1036–1043.
12 J. Albarrán-Velo, V. Gotor-Fernández and I. Lavandera, *Adv. Synth. Catal.*, 2021, **363**, 4096–4108.
13 Y. Peng, D. Li, J. Fan, W. Xu, J. Xu, H. Yu, X. Lin and Q. Wu, *Eur. J. Org. Chem.*, 2020, 821–825.
14 J. S. DeHovitz, Y. Y. Loh, J. A. Kautzky, K. Nagao, A. J. Meichan, M. Yamauchi, D. W. C. MacMillan and T. K. Hyster, *Science*, 2020, **369**, 1113–1118.
15 X. Guo, Y. Okamoto, M. R. Schreier, T. R. Ward and O. S. Wenger, *Chem. Sci.*, 2018, **9**, 5052–5056.
16 K. Mitsukura, M. Suzuki, K. Tada, T. Yoshida and T. Nagasawa, *Org. Biomol. Chem.*, 2010, **8**, 4533–4535.
17 K. Mitsukura, M. Suzuki, S. Shinoda, T. Kuramoto, T. Yoshida and T. Nagasawa, *Biosci., Biotechnol., Biochem.*, 2011, **75**, 1778–1782.
18 X. Li, Y. Hu, J. D. Bailey and B. H. Lipshutz, *Org. Lett.*, 2024, **26**, 2778–2783.
19 W. Zawodny, S. L. Montgomery, J. R. Marshall, J. D. Finnigan, N. J. Turner and J. Clayden, *J. Am. Chem. Soc.*, 2018, **140**, 17872–17877.
20 I. Peñafiel, R. A. W. Dryfe, N. J. Turner and M. F. Greaney, *ChemCatChem*, 2021, **13**, 864–867.
21 J. J. Sangster, R. E. Ruscoe, S. C. Cosgrove, J. Mangas-Sánchez and N. J. Turner, *J. Am. Chem. Soc.*, 2023, **145**, 4431–4437.
22 D. Arnodo, F. De Nardi, S. Parisotto, E. De Nardo, S. Cananà, F. Salvatico, E. De Marchi, D. Scarpi, M. Blangetti, E. G. Occhiato and C. Prandi, *ChemSusChem*, 2024, **17**, e202301243.
23 N. Kesharwani, K. Garima, V. Srivastava, P. P. Singh and P. K. Singh, *Asian J. Org. Chem.*, 2025, **14**, e202400561.
24 N. Halland, A. Braunton, S. Bachmann, M. Marigo and K. A. Jørgensen, *J. Am. Chem. Soc.*, 2004, **126**, 4790–4791.
25 J. J. Feld, K. V. Kowdley, E. Coakley, S. Sigal, D. R. Nelson, D. Crawford, O. Weiland, H. Aguilar, J. Xiong, T. Pilot-Matias, B. DaSilva-Tillmann, L. Larsen, T. Podsadecki and B. Bernstein, *N. Engl. J. Med.*, 2014, **370**, 1594–1603.
26 J. W. Daly, *J. Nat. Prod.*, 1998, **61**, 162–172.
27 W. Chen, L. Ma, A. Paul and D. Seidel, *Nat. Chem.*, 2018, **10**, 165–169.
28 S. Munnuri, A. M. Adebesin, M. P. Paudyal, M. Yousufuddin, A. Dalipe and J. R. Falck, *J. Am. Chem. Soc.*, 2017, **139**, 18288–18294.

This journal is © The Royal Society of Chemistry 2025

Open Access Article. Published on 02 October 2025. Downloaded on 2/8/2026 2:10:41 AM.
This article is licensed under a Creative Commons Attribution-NonCommercial 3.0 Unported Licence.

29 B. Z. Costa, J. L. Galman, I. Slabu, S. P. France, A. J. Marsaioli and N. J. Turner, *ChemCatChem*, 2018, **10**, 4733–4738.
30 E. O'Reilly, C. Iglesias, D. Ghislieri, J. Hopwood, J. L. Galman, R. C. Lloyd and N. J. Turner, *Angew. Chem., Int. Ed.*, 2014, **53**, 2447–2450.
31 B. Chen, R. Li, J. Feng, B. Zhao, J. Zhang, J. Yu, Y. Xu, Z. Xing, Y. Zhao, B. Wang and X. Huang, *J. Am. Chem. Soc.*, 2024, **146**, 14278–14286.
32 J. Davies, S. G. Booth, S. Essafi, R. A. W. Dryfe and D. Leonori, *Angew. Chem., Int. Ed.*, 2015, **54**, 14017–14021.
33 X. Shen, C. Huang, X.-A. Yuan and S. Yu, *Angew. Chem., Int. Ed.*, 2021, **60**, 9672–9679.
34 H. Mao, Y. Zhang, H. Cao, Q. Shi, Y. Lan, J. Chang and B. Zhu, *Org. Chem. Front.*, 2024, **11**, 3204–3213.
35 J.-Y. Zhang, X.-H. Duan, J.-C. Yang and L.-N. Guo, *J. Org. Chem.*, 2018, **83**, 4239–4249.
36 T. Koike and M. Akita, *Inorg. Chem. Front.*, 2014, **1**, 562–576.
37 K. A. Gardner, L. L. Kuehnert and J. M. Mayer, *Inorg. Chem.*, 1997, **36**, 2069–2078.
38 Y. Gao, N. J. DeYonker, E. C. Garrett III, A. K. Wilson, T. R. Cundari and P. Marshall, *J. Phys. Chem. A*, 2009, **113**, 6955–6963.
39 S. Matkhalikova, V. Malikov and S. Y. Yunusov, *Chem. Nat. Compd.*, 1969, **5**, 24–25.
40 M. Khanov, M. Sultanov and M. Egorova, *Farmakol. Alkaloidov Serdech. Glikoyidov*, 1971, 210–212.
41 A. Kotland, F. Accadbled, K. Robeyns and J.-B. Behr, *J. Org. Chem.*, 2011, **76**, 4094–4098.
42 S. A. Johari, M. Mohtar, S. A. Syed Mohammad, R. Sahdan, Z. Shaameri, A. S. Hamzah and M. F. Mohammat, *BioMed Res. Int.*, 2015, **2015**, 823829.
43 C. R. B. Swanson, L. Gourbeyre, G. J. Ford, P. Clapés and S. L. Flitsch, *J. Am. Chem. Soc.*, 2025, **147**, 6067–6075.
44 C. R. B. Swanson, G. J. Ford, A. P. Mattey, L. Gourbeyre and S. L. Flitsch, *ACS Cent. Sci.*, 2023, **9**, 103–108.
45 E. Speckmeier, T. G. Fischer and K. Zeitler, *J. Am. Chem. Soc.*, 2018, **140**, 15353–15365.
46 K. Sun, C. Ge, X. Chen, B. Yu, L. Qu and B. Yu, *Nat. Commun.*, 2024, **15**, 9693.
47 C. Gao, J. Zeng, X. Zhang, Y. Liu and Z.-p. Zhan, *Org. Lett.*, 2023, **25**, 3146–3151.
48 S. Dutta, J. E. Erchinger, F. Strieth-Kalthoff, R. Kleinmans and F. Glorius, *Chem. Soc. Rev.*, 2024, **53**, 1068–1089.
49 L. Schlosser, D. Rana, P. Pflüger, F. Katzenburg and F. Glorius, *J. Am. Chem. Soc.*, 2024, **146**, 13266–13275.